Journal of Neuroscience Research

Journal of Neuroscience Research 91:1076–1083 (2013)

Net Increase of Lactate and Glutamate Concentration in Activated Human Visual Cortex Detected With Magnetic Resonance Spectroscopy at 7 Tesla

Benoît Schaller,[1] Ralf Mekle,[2] Lijing Xin,[1] Nicolas Kunz,[3] and Rolf Gruetter[1,4,5]★

[1]Laboratory of Functional and Metabolic Imaging, Ecole Polytechnique Federale de Lausanne, Lausanne, Switzerland
[2]Physikalisch-Technische Bundesanstalt, Medical Physics, University Hospitals of Geneva, Geneva, Switzerland
[3]Division of Development and Growth, Department of Pediatrics, University Hospitals of Geneva, Geneva, Switzerland
[4]Department of Radiology, University Hospitals of Geneva, Geneva, Switzerland
[5]Department of Radiology, University Hospitals of Lausanne, Lausanne, Switzerland

After the landmark studies reporting changes in the cerebral metabolic rate of glucose (CMR_{Glc}) in excess of those in oxygen (CMR_{O2}) during physiological stimulation, several studies have examined the fate of the extra carbon taken up by the brain, reporting a wide range of changes in brain lactate from 20% to 250%. The present study reports functional magnetic resonance spectroscopy measurements at 7 Tesla using the enhanced sensitivity to study a small cohort (n = 6). Small increases in lactate (19% ± 4%, $P < 0.05$) and glutamate (4% ± 1%, $P < 0.001$) were seen within the first 2 min of activation. With the exception of glucose (12% ± 5%, $P < 0.001$), no other metabolite concentration changes beyond experimental error were significantly observed. Therefore, the present study confirms that lactate and glutamate changes during physiological stimulation are small (i.e. below 20%) and shows that the increased sensitivity allows reproduction of previous results with fewer subjects. In addition, the initial rate of glutamate and lactate concentration increases implies an increase in CMR_{O2} that is slightly below that of CMR_{Glc} during the first 1–2 min of activation.

Key words: lactate; oxidative metabolism; visual stimulation; in vivo ^{1}H-NMR spectroscopy; neurotrans mitters

At physiological resting state, cerebral metabolic rate of glucose (CMR_{Glc}), cerebral blood flow (CBF), and cerebral metabolic rate of oxygen (CMR_{O2}) are generally considered to be tightly coupled (Fox and Raichle, 1986; Fox et al., 1988), with energy needs supported mainly by glucose oxidation. Nonetheless, during visual stimulation, significant uncoupling of the changes of CMR_{Glc} (ΔCMR_{Glc} = 22–50%), of CBF (ΔCBF = 30–65%), and of CMR_{O2} (ΔCMR_{O2} = 5–30%) have been reported for the human brain (Fox and Raichle, 1986; Fox et al., 1988; Chen et al., 1993; Madsen et al., 1995; Kim and Ugurbil, 1997; Davis et al., 1998; Liu et al., 2004; Zhu et al., 2009; Leithner et al., 2010; Lin et al., 2010; Wey et al., 2011). Such uncoupling during physiological stimulation forms the basis of the blood-oxygen-level-dependent effect (BOLD) used in functional magnetic resonance imaging (fMRI; Lin et al., 2010, and references therein). Furthermore, Fox et al. (1988) proposed that increased neuronal activity requires only small amounts of chemical energy produced by oxidative phosphorylation. However, given the high ATP yield of oxidative phosphorylation, glucose oxidation may still be considered as a major source of energy during physiological stimulation (Rothman et al., 2003). Aerobic glycolysis (i.e., production of lactate) has thus been suggested to explain the observed uncoupling.

Investigation of brain lactate concentration changes during stimulation has led to variable results in the human brain such as a major increase (Prichard et al., 1991; Sappey-Marinier et al., 1992), a transient increase (Frahm et al., 1996), or the absence of changes

Contract grant sponsor: Swiss National Science Foundation; Grant number: 131087; Contract grant sponsor: Centre d'Imagerie BioMédicale (CIBM) of the University of Lausanne (UNIL), The Swiss Federal Institute of Technology Lausanne (EPFL), The University of Geneva (UniGe), The Centre Hospitalier Universitaire Vaudois (CHUV), The Hôpitaux Universitaires de Genéve (HUG), The Leenaards and the Jeantet Foundations.

★Correspondence to: Rolf Gruetter, Ecole Polytechnique Federale de Lausanne, SB-IPMC-LIFMET, Station 6, 1015 Lausanne, Switzerland. E-mail: rolf.gruetter@epfl.ch

Received 3 July 2012; Accepted 21 November 2012

Published online 1 February 2013 in Wiley Online Library (wileyonlinelibrary.com). DOI: 10.1002/jnr.23194

(Merboldt et al., 1992; Sandor et al., 2005). However, a recent study involving 12 subjects using the high sensitivity of magnetic resonance spectroscopy (MRS) at 7 Tesla (T) and optimized functional MRS (fMRS) methodology reported a small but sustained increase of lactate during visual stimulation (23% ± 5%; Mangia et al., 2007). An optimized implementation of the MRS sequence stimulated-echo acquisition mode (STEAM) sequence (Tkac and Gruetter, 2005, and references therein) that allows recording signal at short echo times was used in that study. More recently, two studies have also shown a lactate increase of 50% ± 5% (n = 12 [Lin et al., 2010] at 3T) and 10% ± 6% (n = 8 [Lin et al., 2012] at 7T) during visual stimulation using STEAM.

All of the aforementioned studies were performed at B_0 fields lower than 7 T, except for those of Mangia et al. (2007) and Lin et al. (2012), which used STEAM localization that incurs a nearly twofold lower sensitivity than theoretically possible with a spin-echo-based sequence (Mlynarik et al., 2006; Mekle et al., 2009). For all studies of dynamic concentration changes using fMRS, a reliable measurement of the time evolution is advantageous for the characterization of the very small transient changes (about 0.2 μmol/g) used in the subsequent analysis of metabolic rates. Therefore, measurements with the highest possible sensitivity are desirable. In this study, proton MR spectra were acquired with the spin-echo full-intensity acquired localized (SPECIAL) sequence, allowing for full signal acquisition at short echo time (TE; Mlynarik et al., 2006; Mekle et al., 2009) in combination with the use of a high magnetic field system (7T) and the advantages that it provides (Tkac and Gruetter, 2005).

During physiological stimulation, brain cells require energy for neuronal firing and the replenishment of neurotransmitter, of which glutamate is the most prominent (Fonnum, 1984; Erecinska and Silver, 1990). Glucose is the primary substrate for energy metabolism and an increase in its metabolism during functional activity leads to an incremental increase in energy production (ATP) mainly via the TCA cycle.

Therefore, the aim of the present study was to use the enhanced sensitivity of a spin-echo-based acquisition technique to characterize metabolite changes during functional activation in general and to confirm the results from a previous study (Mangia et al., 2007; Lin et al., 2012) in fewer subjects.

MATERIALS AND METHODS

MR Protocol

Ten healthy volunteers (one female, nine males, 20–28 years) participated in the study and gave informed consent according to a procedure approved by the local ethics committee. The experiments were performed on a 7-T/68-cm (Siemens Healthcare, Erlangen, Germany) scanner with the use of a home-built quadrature transmit/receive surface coil (diameter 13 cm). All of the participants were subjected to the same experiment and functional paradigm. Anatomical images were acquired using a multislice gradient echo imaging sequence. A "localizer" fMRI experiment was then performed using a multislice EPI sequence similar to the one described by van der Zwaag et al. (2009). The activation paradigm consisted of a 9-Hz reversed black–grey checkerboard, alternating with a black screen with the following timing: 10 sec on–20 sec off (total acquisition time [TA] 2 min 30 sec). The stimulus was presented on a screen covering the back of the magnet bore. Based on anatomical landmarks, the MRS voxel (VOI = 20 × 22 × 20 mm^3) was placed either inside the BOLD-activated volume (primary visual cortex in both hemispheres, referred to as "activated tissue"; n = 6), or outside the BOLD-activated volume (above the primary visual cortex, referred to as "nonactivated tissue"; n = 4). A localized calibration of the RF transmitter voltage was then performed for the selected VOI. All first- and second-order shim terms were adjusted using FAST(EST)MAP (Gruetter, 1993; Gruetter and Tkac, 2000) to minimize B_0 homogeneities over the volume of interest.

During the fMRS measurements, ^{1}H spectra were continuously acquired. A SPECIAL localization sequence (Mlynarik et al., 2006; TR/TE = 5,000/6 msec, BW = 4,000 Hz, vector size = 2,048 pts, carrier frequency of the pulses set to 2.35 ppm off-resonance from water peak) with two averages was used. The SPECIAL sequence was preceded by VAPOR water suppression (WS) interleaved with blocks of outer volume saturation (OVS) used to minimize the water signal and lipid signals from extracerebral fat tissue (Tkac and Gruetter, 2005). In addition to the optimization of the flip angles of the WS pulses for each subject, the OVS bands were carefully placed to minimize lipid contamination of the ^{1}H spectra. The functional paradigm employed for the fMRS experiment consisted of the same black–grey checkerboard as that employed for the "localizer" experiment, but the timing was different: five periods of 5 min (off–on–off–on–off, TA = 25 min) were acquired. A red cross was placed in the center of the screen, and subjects were asked to report rotations of the fixation cross via a button press.

Data Processing

The acquired free induction decays (FIDs) were separately stored for each pair of scans. Spectral quality was such that neither additional water removal nor baseline correction was necessary or applied. After Fourier transformation, spectra were frequency corrected to compensate for small B_0 drift as described by Tkac and Gruetter (2005). We checked rigorously for lipid contamination. Specifically, the ratio of the height of the NAA peak to the height of the sum of macromolecules and lipid resonances (at 0.89 ppm, 1.22 ppm, 1.41 ppm, and 1.7 ppm) was allowed to deviate by less than 20% of the mean value. Spectra that did not satisfy this condition were discarded. Finally, prior to quantification, spectra were averaged into blocks of various sizes following three approaches, as described below.

In the first approach, MR spectra were individually analyzed, with FIDs averaged into blocks of six scans each. A mean time course was obtained by averaging the metabolite concentrations across all six subjects for whom the MRS voxel was placed in activated tissue. To reduce temporal fluctua-

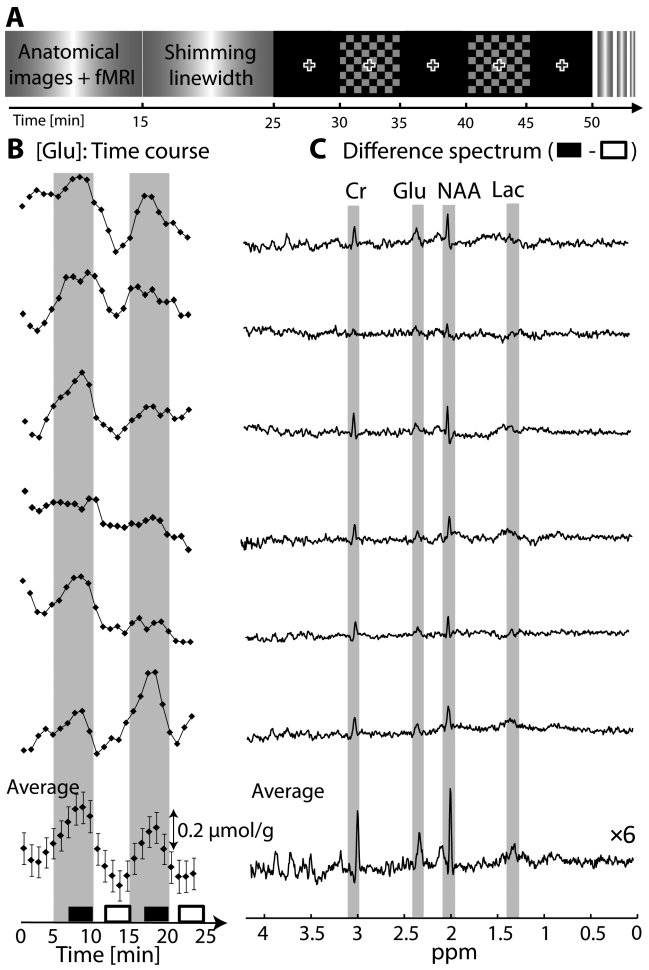

Fig. 1. **A**: The complete acquisition protocol used in this study lasted for about 55 min for each subject. An initial gradient echo sequence and a brief "localizer" fMRI experiment were followed by a shimming procedure using FAST(EST)MAP. The fMRS experiment lasted for 25 min and consisted of rest periods (black screen) alternating with activation periods (reversed black–grey checkerboard). Time courses of glutamate during the functional paradigm (**B**) in the activated tissue for six individual subjects and for the summed subjects and their difference spectra (**C**). Moving average with a kernel of 4 scans (24 data points) was applied after quantification. Data are reported as mean values µmol/g. Error bars correspond to the mean of CRLB divided by the square root of the number of points. Difference spectra were obtained by subtracting the summed ^{1}H spectra acquired during stimulation (black blocks) and rest (white blocks) periods. Metabolite peaks were observed above the noise level of the difference spectrum (line broadening of 1 Hz was applied to all spectra).

tions, a moving average with a kernel of four scans was applied after quantification for the plot of individual time courses. In addition, for each individual subject, metabolite concentration changes between activation and rest periods (time course analysis) were obtained by comparing the last 40 scans of the two activation blocks to the last two rest blocks, i.e., ^{1}H spectra acquired during the last 3.3 min of each 5-min block. The time course analysis of the metabolite concentration changes was performed by using a two-way ANOVA with Bonferroni posttest correction. The same averaged spectra were used to obtain individual difference spectra.

In the second approach, MR spectra were combined across subjects prior to quantification to perform a group analysis. Each time point was the average of 24 scans (4 scans/subject, n = 6) for the activated tissue, and an average of 16 scans was used (4 scans/subject, n = 4) for the nonactivated tissue, leading to 75 points in the mean time course. A moving average with four scans kernel was applied after quantification for the plot of the mean time courses. A comparison of the time courses from voxels placed outside (nonactivated tissue) and inside (activated tissue) the strongly activated area was used to confirm that the metabolite concentration changes were related to the visual stimulation.

Finally, a difference spectrum was calculated by subtracting the mean activated spectrum (80 scans/subject, n = 6, NT = 480 scans) from the mean rest spectrum (NT = 480 scans) following the same procedure as for the individual difference spectra. To remove the BOLD effect from the spectra during activation and compensate for the longer T_2^* (Zhu and Chen, 2001), an additional line broadening (0.45 Hz) was applied to the mean activated spectrum prior to Fourier transformation. The resulting BOLD-free difference spectrum was then quantified with LCModel (Provencher, 1993).

All spectra were fitted and quantified with LCModel using a basis set including simulated spectra of 20 metabolites with published values for chemical shift and J-coupling and an experimentally measured macromolecule baseline, as described by Mekle et al. (2009). The LCModel analyses were carried out from 0.2 ppm to 4.2 ppm. The Cramér-Rao lower bound (CRLB), which gives a measure for the precision of metabolite quantification assuming that the model function is correct, was used as a marker of quantification reliability (Provencher, 1993; Cavassila et al., 2001; Mlynarik et al., 2007). Only metabolites with CRLBs below 30% were reported, following Mangia et al. (2007).

RESULTS

After adjustment of first- and second-order shim terms using FAST(EST)MAP, the average water linewidths in the VOI was 12.9 ± 0.7 Hz (mean ± SD, n = 6). In vivo ^{1}H-MR spectra were continuously acquired during the functional paradigm (Fig. 1A). Physiological motion such as subject motion or small breathing resulted in a mean frequency drift of B_0 = 2 ± 1 Hz (mean ± SD, n = 6) during the fMRS experiment (25 min). The high stability of the scanner yielded highly reproducible spectra, and no phase correction was required. A B_0 correction was applied for all ^{1}H spectra before summation and prior to metabolite quantification. The water residual was generally minimized to below the height of the NAA peak. Thus, lipid contamination can be considered to be negligible in these spectra. Less than 6% of the spectra acquired with two averages were discarded (criterion is described in Materials and Methods). The ratio of the height of the NAA peak (2.01 ppm) to the standard deviation of the noise in a metabolite-free region of the spectrum

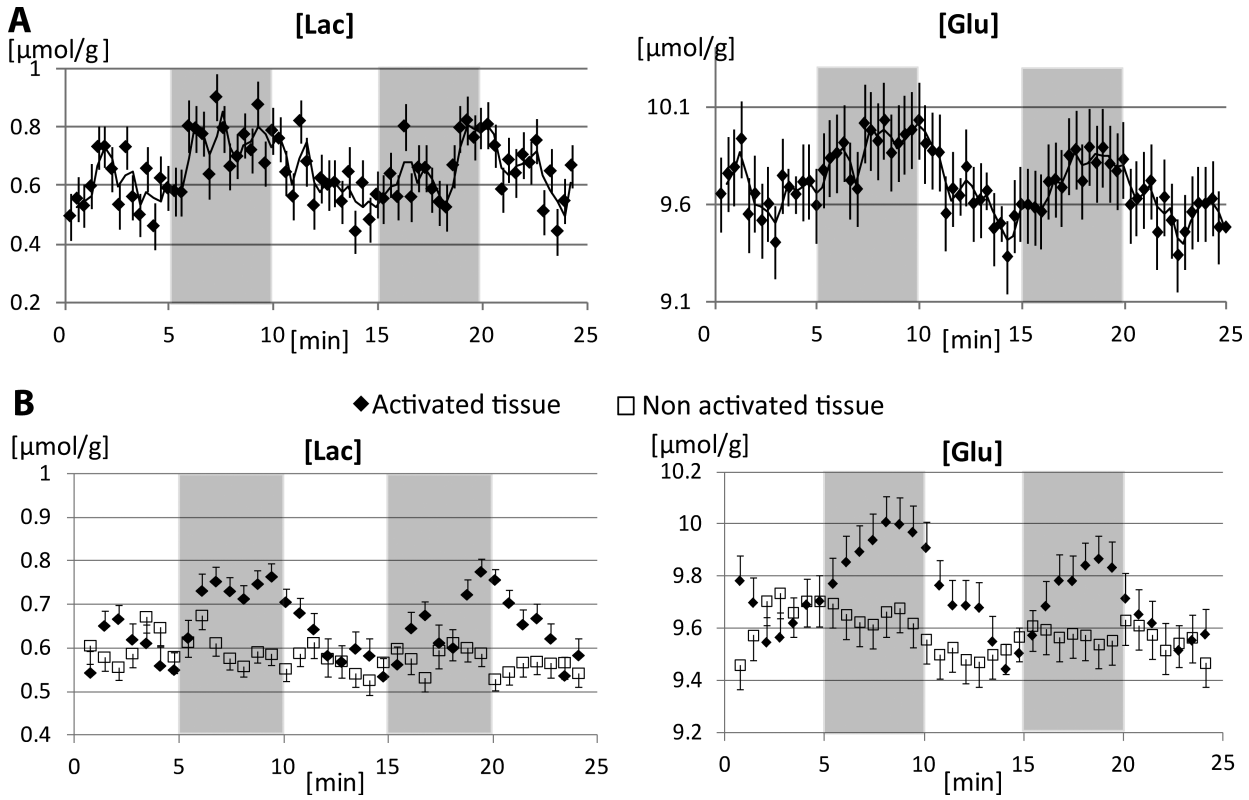

Fig. 2. **A**: Group analysis with time courses of metabolite concentrations (24 scans/data point, 75 data points) during the functional paradigm. Error bars correspond to CRLB (µmol/g). **B**: Overlap of the time courses of lactate and glutamate concentration when the voxel was placed inside (activated tissue, 24 scans/data point, n = 6; lozenges) or outside (nonactivated tissue, 16 scans/data point, n = 4; squares) the BOLD activated volume. Moving average with a kernel of 4 scans (36 data points) was applied after quantification. Data are reported as the mean metabolite concentration in µmol/g. Error bars correspond to the mean of CRLB divided by the square root of the number of points. Relative increases of lactate (19% ± 4%, $P < 0.001$) and glutamate (4% ± 1%, $P < 0.05$) were found (n = 6, mean ± SEM).

(9–10 ppm), for a pair of scans, gave a signal-to-noise ratio (SNR) of 55 ± 4 (mean ± SD, n = 6).

To study the metabolite changes of a given individual subject within activated tissue, time points were averaged at a temporal resolution of 30 sec (NT = 6), allowing quantification of lactate and glutamate with CRLB lower than 30% and 4%, respectively. The application of a moving average reduced the time resolution to 60 sec, rendering the changes of glutamate concentration in the visual cortex visually apparent for each subject (Fig. 1B). The changes were more apparent when averaging the time courses over subjects (Fig. 1B, bottom). The increase in glutamate concentration was observed within the first few minutes of activation.

When comparing activation with rest for each subject, relative increases of the lactate concentration by 19% ± 4% ($P < 0.05$, n = 6) and of the glutamate concentration by 4% ± 1% ($P < 0.001$, n = 6) were found. In absolute concentration, the lactate increased by 0.12 ± 0.03 µmol/g, with a mean control concentration of 0.61 ± 0.04 µmol/g, and glutamate increased by 0.33 ± 0.05 µmol/g, with a mean control concentration of 9.6 ± 0.2 µmol/g. In addition, glucose decreased significantly by 11% ± 3% ($P < 0.001$, n = 6), and aspartate had a tendency to decrease by 7% ± 3% ($P > 0.05$, n = 6). To verify the overall spectral stability and reproducibility of the experiment, difference spectra between the activation and the rest periods were generated for individual subjects (Fig. 1C). A BOLD effect on metabolite resonances was observed in the difference spectra by the presence of a residual Cr and NAA signal above the noise level induced by a linewidth narrowing during activation. The linewidth-narrowing effect resulted in an average increase of the Cr peak height of about 3% between the activation periods and the following rest periods (data not shown). Note that increased glutamate was evident in all difference spectra in Figure 1C.

To investigate further the aforementioned metabolite changes, time points were averaged over the activated tissue, giving a native time resolution of 20 sec (Fig. 2A). This allowed quantification of 16 metabolites with CRLB below 30% (Asp, Cr, PCr, GABA, Glc, Gln, Glu, GSH, GPC, Ins, Lac, NAA, NAAG, PE, Scyllo, Tau, GPC + PCho; Table I). In particular, CRLB was below 18% for lactate and below 3% for glutamate. These CRLBs translated into an average

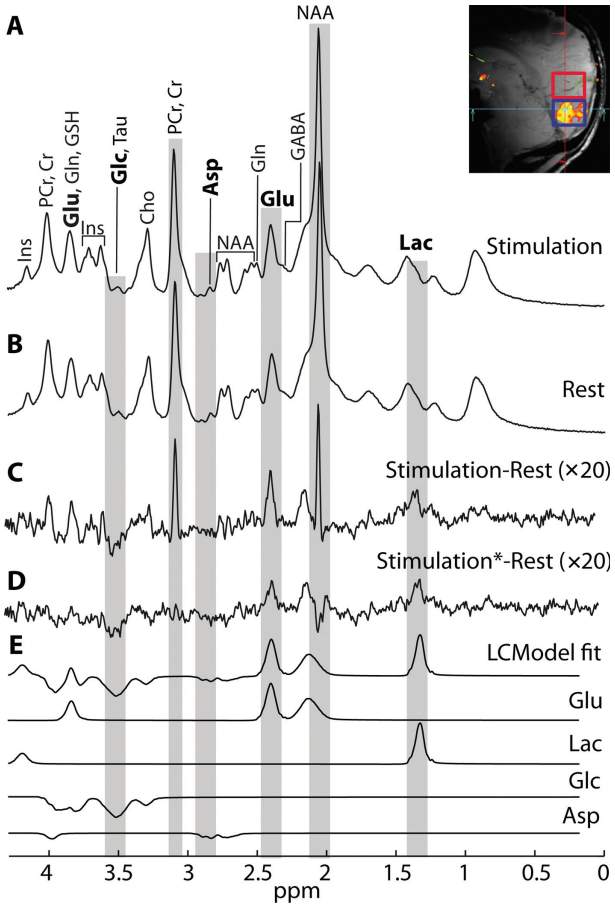

Fig. 3. Summed ^{1}H spectra acquired during activation (**A**) and rest (**B**) periods (n = 6, 480 scans) were subtracted to yield the difference spectrum (**C**). An additional line broadening (asterisk) of 0.45 Hz was applied to the summed activated spectrum to correct for the BOLD effect on metabolite linewidth (**D**). LCModel analysis of the corrected difference spectrum and the corresponding fits of Glu, Lac, Glc, and Asp. (**E**) LCModel metabolite quantification for Glu and Lac was 0.28 ± 0.01 μmol/g and 0.18 ± 0.01 μmol/g (concentration ± CRLB), respectively. **Inset**: Overlap of the functional map and the anatomical image was used to place the voxel of interest (VOI = 20 × 22 × 20 mm^3) inside (bottom voxel, activated tissue) or outside (top voxel, nonactivated tissue) the BOLD activated volume.

precision on the order of 0.2 μmol/g for an average of 24 scans. The application of a moving average shift of 2 scans reduced the time resolution to 40 sec, and the ensuing time courses depicted an increase of lactate (20% ± 2%) and glutamate (3.4% ± 0.1%) within approximately the first 2 min of the activation periods (lozenges in Fig. 2B). An apparent steady-state was reached, which was maintained until the end of the activation period. Typically, a return to baseline during the rest period was observed. Unlike the time courses of the activated tissue, the nonactivated tissue presented a relatively stable lactate and glutamate concentration (squares in Fig. 2B). Difference spectra for the nonactivated tissue were also obtained (not shown) and exhibited noisy flat residuals.

TABLE I. Mean Metabolite Concentrations During the Rest Periods (μmol/g) and the mean Concentration Changes (μmol/g and Percentage) During the Activation Periods (n = 6)[†]

	Metabolite concentration at rest (μmol/g)	Concentration change	
		Absolute (μmol/g)	Percentage (%)
Lac	0.61 ± 0.04⋆	0.12 ± 0.03⋆	19 ± 4⋆
Glu	9.6 ± 0.2⋆	0.33 ± 0.05⋆	4 ± 1⋆
Glc	2.0 ± 0.2⋆	−0.23 ± 0.04⋆	−11 ± 3⋆
Asp	1.6 ± 0.2	−0.10 ± 0.04	−7 ± 3
Cr	3.9 ± 0.1	0.04 ± 0.04	1 ± 1
PCr	4.1 ± 0.1	0.07 ± 0.03	2 ± 1
GABA	1.2 ± 0.1	0.00 ± 0.01	0 ± 1
Gln	2.3 ± 0.1	0.04 ± 0.01	2 ± 1
GSH	0.7 ± 0.1	−0.01 ± 0.02	−2 ± 3
GPC	0.6 ± 0.1	0.05 ± 0.01	4 ± 1
Ins	6.0 ± 0.2	−0.01 ± 0.05	0 ± 1
NAA	12.0 ± 0.2	0.08 ± 0.04	1 ± 0
NAAG	1.5 ± 0.1	0.01 ± 0.04	0 ± 3
PE	2.6 ± 0.1	0.00 ± 0.03	0 ± 1
Scyllo	0.2 ± 0.0	0.02 ± 0.01	13 ± 4
Tau	0.9 ± 0.1	0.07 ± 0.03	7 ± 3
GPC + PCho	0.8 ± 0.0	0.02 ± 0.01	2 ± 1
Tot Cr	8.0 ± 0.0	0.10 ± 0.04	1 ±1
Tot NAA	10.7 ± 0.8	0.07 ± 0.04	1 ± 0

[†]Sixteen metabolites were quantified with LCModel with CRLB below 30% (NT = 24): lactate (Lac), glutamate (Glu), glucose (Glc), aspartate (Asp), creatine (Cr), phosphocreatine (PCr), γ-aminobutyrate (GABA), glutamine (Gln), glutathione (GSH), glycerophosphocholine (GPC), myoinositol (Ins), N-acetylaspartate (NAA), N-acetylaspartylglutamate (NAAG), phosphoethanolamine (PE), scylloinositol (Scyllo), taurine (Tau), glycerophosphocholine + phosphocholine (GPC + PCho), total creatine (tot Cr), and total N-acetylaspartate (tot NAA). The concentrations changes were obtained from the time group analysis (NT = 80 scans for rest and for activation periods, n = 6). Data are expressed as mean ± SEM. ⋆Metabolites with significant changes ($P < 0.05$, two-way ANOVA with Bonferroni posttest correction).

Neither line broadening from a BOLD effect nor metabolite signal changes were detected.

To demonstrate further the presence of small metabolite changes ascertained by LCModel as described above, a difference spectrum was obtained from the average of the six activated tissue (Fig. 3). After correction for the BOLD effect, lactate and glutamate signal changes were above the noise level and were quantified with CRLBs below 25%.The quantification of the difference spectrum (Fig. 3E) yielded a relative increase of glutamate and lactate of 0.28 ± 0.01 μmol/g and 0.18 ± 0.01 μmol/g, respectively. The CRLBs obtained from the quantification imply an unequivocal detection of metabolite changes in the difference spectrum.

DISCUSSION

This study reports metabolite concentration changes of lactate and glutamate for a small number of subjects (n = 6) during physiological stimulation of the visual cortex. ^{1}H-MR spectra were acquired with high sensitivity (SNR = 55 ± 4, relative to the height of the

NAA peak, NT = 2), which allowed quantification of metabolite of interests with CRLB below 18% (NT = 24). The analyses were based on individual time courses using a moving average (Fig. 1) or were based on group analysis by averaging spectra across subjects (Fig. 2) or were performed by analyzing the difference spectra between activation and rest (Fig. 3). Results consistently showed an increase of lactate by 19% ± 3% ($P < 0.05$) and of glutamate by 4% ± 1% ($P < 0.001$), in agreement with recent studies (Mangia et al., 2007; Lin et al., 2012).

Based on the fMRI "localizer" scan, the voxel was placed in a highly activated area of the activated tissue. Linewidth changes, induced by the BOLD effect (Zhu and Chen, 2001), were consistently observed for each subject in the difference spectrum (Fig. 1C). The flat residual of each difference spectrum illustrated the overall stability and reproducibility of the experiment. In our study, the region of 1.3–1.5 ppm was devoid of any observable variation (except for potential metabolite changes), and lipid resonances were suppressed to a level that is unlikely to affect the observed changes in lactate or other metabolites. In contrast, when the voxel was placed above the primary visual cortex for the nonactivated tissue, the difference spectrum yielded a flat baseline, and no BOLD effect was present (data not shown). The comparison between the metabolite time courses of the activated tissue and the nonactivated tissue confirmed that these metabolite changes occurred only where neuronal activation took place (Fig. 2B). However, minor but statistically nonsignificant metabolite changes were observed in the time courses of the nonactivated tissue, which might be induced by some unwanted signal change resulting from the proximity of the VOI with respect to the activated area. Therefore, it can be inferred that substantial metabolite signal changes occurred only in the inferior voxel (Fig. 3, inset) and were directly related to the activation of the primary visual cortex.

The present study differs in that respect from all previous reports by not focusing primarily on lactate changes or larger subject groups (Prichard et al., 1991; Merboldt et al., 1992; Sappey-Marinier et al., 1992; Frahm et al., 1996; Sandor et al., 2005; Mangia et al., 2007; A.L. Lin et al., 2010; Y. Lin et al., 2012). The high sensitivity of the measurements allowed the study of metabolite changes during functional activity with relatively few subjects (n = 6) and a small number of averages (NT = 24), a substantial improvement compared with a previous study (n = 12, NT = 48; Mangia et al., 2007) and consistent with the nearly twofold increase in sensitivity provided by SPECIAL over STEAM (Mlynarik et al., 2006; Mekle et al., 2009). Sixteen metabolites were reliably quantified with CRLB below 30% (Table I), and their absolute concentrations were in agreement with published metabolite concentrations at 7 T (Mangia et al., 2006; Mekle et al., 2009; Emir et al., 2012). Although the two are qualitatively similar, our study is closer to the study by Mangia et al. (2007) than that by Lin et al. (2012), who reported a transient and twofold smaller relative increase of lactate during stimulation. In addition, Lin et al. (2012) reported concentration changes for glutathione, aspartate, glutamine, and glycine (2–11%). With the exception of aspartate, whose change was near significance in our study, and glucose, the other metabolites did not reach significance (Table I).

Several experimental reasons may underlie differences in the reported changes of lactate following visual stimulation (Prichard et al., 1991; Merboldt et al., 1992; Sappey-Marinier et al., 1992; Frahm et al., 1996; Sandor et al., 2005; Mangia et al., 2007; A.L. Lin et al., 2010; Y. Lin et al., 2012). First, different acquisition sequences were employed (ISIS, PRESS, STEAM, SPECIAL). Second, different stimulation paradigms were used, which directly affect processing of light stimuli by the retina. Consequently, the visual cortex might have been differentially stimulated, exciting different neuronal populations, which would lead to different stimulus response properties (Zeki, 1990, 2003; Olavarria et al., 1992; Grill-Spector et al., 1999; Gazzaniga, 2004; Grill-Spector and Malach, 2004; Wandell et al., 2009). Third, we cannot exclude the possibility that the smaller voxel used here or higher sensitivity contributes to differences in the metabolite changes compared with studies at lower field. To take these issues into account, the use of a short TE combined with high magnetic field strength (7 T) and the full magnetization available from the small VOI ($20 \times 22 \times 20$ mm^3), by using the spin echo-based SPECIAL sequence, allowed a substantial gain in sensitivity compared with previous studies. Note that differences in relative lactate changes between studies may be due to different baseline concentrations. Therefore, we provided quantification of metabolite changes in absolute concentration and percentage changes (Table I), which are consistent with recent studies at 7 T (Mangia et al., 2007; Lin et al., 2012).

It is of interest to note that the physiological stimulation led to a new steady state for lactate and glutamate after the first minutes of activation (Fig. 2). The plots of glutamate and lactate time courses during the stimulation period clearly illustrate a new steady-state level reached by the metabolites and do not suggest a continuous increase of glutamate and lactate during physiological stimulation. After stimulation, the fall of glutamate below the initial baseline level might be caused by a slower return of CMR_{O2} to the baseline compared with CBF, which is believed to be responsible of the poststimulus BOLD undershoot (Frahm et al., 1996; Kruger et al., 1996; Lu et al., 2004; Yacoub et al., 2006).

The initial rise of lactate and glutamate after stimulus onset results in a net increase of carbon in tissue that would otherwise be metabolized to CO_2 and, therefore, implies a transient uncoupling of CMR_{Glc} from CMR_{O2}. The uncoupling of the changes of CMR_{O2} and CMR_{Glc} has already been demonstrated in positron emission studies (PET) studies (Fox and Raichle, 1986; Fox et al., 1988; Madsen et al., 1995). In contrast, MR studies using a BOLD effect have reported both linear and nonlinear coupling for human and animal studies (Hyder et al.,

2001; Rothman et al., 2003; Dienel and Cruz, 2004; Liu et al., 2004; Leithner et al., 2010; Lin et al., 2010; Wey et al., 2011), which has been attributed to different experimental conditions, stimuli, paradigms, frequencies, and brain regions (Vafaee and Gjedde, 2000, 2004; Rothman et al., 2003; Zhu et al., 2009). Note, however, that, despite the uncoupling that undoubtedly must have occurred, an energy balance calculation (not shown) indicates that the energy demands during neuronal activation are largely met through oxidative metabolism at all times.

In addition to PET and MR studies, flavoprotein fluorescence imaging has gained interest recently as a powerful imaging tool for visualizing cortical activity and investigating neuronal activity (Reinert et al., 2007). The early and rapid increase of oxidative metabolism observed with flavoprotein imaging within the first minute of stimulation (Reinert et al., 2007; Sirotin and Das, 2010) may indicate that CMR_{O2} increases substantially, but this does not affect the conclusion from the study, which is that an uncoupling must occur transiently.

We conclude that metabolite concentration changes in the visual cortex during visual activation are very small (0.1–0.3 μmol/g), yet can be detected at 7 T with a small number of subjects (n = 6), which opens the possibility of assessing smaller activated VOI. We further conclude that the early transient changes of the metabolite concentrations likely imply a transient mismatch between CMR_{O2} and CMR_{Glc}, the magnitude of which remains to be determined.

ACKNOWLEDGMENTS

The authors declare no conflict of interest. This work was supported by the Centre d'Imagerie Bio-Médicale (CIBM) of the University of Lausanne (UNIL), the Swiss Federal Institute of Technology Lausanne (EPFL), the University of Geneva (UniGe), the Centre Hospitalier Universitaire Vaudois (CHUV), the Hôpitaux Universitaires de Genéve (HUG) and the Leenaards and the Jeantet Foundations and by a Swiss National Science grant to R. Gruetter.

REFERENCES

Cavassila S, Deval S, Huegen C, van Ormondt D, Graveron-Demilly D. 2001. Cramer-Rao bounds: an evaluation tool for quantitation. NMR Biomed 14:278–283.

Chen W, Novotny EJ, Zhu XH, Rothman DL, Shulman RG. 1993. Localized ^{1}H NMR measurement of glucose consumption in the human brain during visual stimulation. Proc Natl Acad Sci U S A 90:9896–9900.

Davis TL, Kwong KK, Weisskoff RM, Rosen BR. 1998. Calibrated functional MRI: mapping the dynamics of oxidative metabolism. Proc Natl Acad Sci U S A 95:1834–1839.

Dienel GA, Cruz NF. 2004. Nutrition during brain activation: does cell-to-cell lactate shuttling contribute significantly to sweet and sour food for thought? Neurochem Int 45:321–351.

Emir UE, Auerbach EJ, Van De Moortele PF, Marjanska M, Ugurbil K, Terpstra M, Tkac I, Oz G. 2012. Regional neurochemical profiles in the human brain measured by ^{1}H MRS at 7 T using local B_1 shimming. NMR Biomed 25:152–160.

Erecinska M, Silver IA. 1990. Metabolism and role of glutamate in mammalian brain. Prog Neurobiol 35:245–296.

Fonnum F. 1984. Glutamate: a neurotransmitter in mammalian brain. J Neurochem 42:1–11.

Fox PT, Raichle ME. 1986. Focal physiological uncoupling of cerebral blood flow and oxidative metabolism during somatosensory stimulation in human subjects. Proc Natl Acad Sci U S A 83:1140–1144.

Fox PT, Raichle ME, Mintun MA, Dence C. 1988. Nonoxidative glucose consumption during focal physiologic neural activity. Science 241:462–464.

Frahm J, Kruger G, Merboldt KD, Kleinschmidt A. 1996. Dynamic uncoupling and recoupling of perfusion and oxidative metabolism during focal brain activation in man. Magn Reson Med 35:143–148.

Gazzaniga MS, editor. 2004. The cognitive neurosciences III. Cambridge, MA: MIT Press. p303–312.

Grill-Spector K, Malach R. 2004. The human visual cortex. Annu Rev Neurosci 27:649–677.

Grill-Spector K, Kushnir T, Edelman S, Avidan G, Itzchak Y, Malach R. 1999. Differential processing of objects under various viewing conditions in the human lateral occipital complex. Neuron 24:187–203.

Gruetter R. 1993. Automatic, localized in vivo adjustment of all first- and second-order shim coils. Magn Reson Med 29:804–811.

Gruetter R, Tkac I. 2000. Field mapping without reference scan using asymmetric echo-planar techniques. Magn Reson Med 43:319–323.

Hyder F, Kida I, Behar KL, Kennan RP, Maciejewski PK, Rothman DL. 2001. Quantitative functional imaging of the brain: towards mapping neuronal activity by BOLD fMRI. NMR Biomed 14:413–431.

Kim SG, Ugurbil K. 1997. Comparison of blood oxygenation and cerebral blood flow effects in fMRI: estimation of relative oxygen consumption change. Magn Reson Med 38:59–65.

Kruger G, Kleinschmidt A, Frahm J. 1996. Dynamic MRI sensitized to cerebral blood oxygenation and flow during sustained activation of human visual cortex. Magn Reson Med 35:797–800.

Leithner C, Royl G, Offenhauser N, Fuchtemeier M, Kohl-Bareis M, Villringer A, Dirnagl U, Lindauer U. 2010. Pharmacological uncoupling of activation induced increases in CBF and CMR_{O2}. J Cereb Blood Flow Metab 30:311–322.

Lin AL, Fox PT, Hardies J, Duong TQ, Gao JH. 2010. Nonlinear coupling between cerebral blood flow, oxygen consumption, and ATP production in human visual cortex. Proc Natl Acad Sci USA 107:8446–8451.

Lin Y, Stephenson MC, Xin L, Napolitano A, Morris PG. 2012. Investigating the metabolic changes due to visual stimulation using functional proton magnetic resonance spectroscopy at 7 T. J Cereb Blood Flow Metab (in press).

Liu ZM, Schmidt KF, Sicard KM, Duong TQ. 2004. Imaging oxygen consumption in forepaw somatosensory stimulation in rats under isoflurane anesthesia. Magn Reson Med 52:277–285.

Lu H, Golay X, Pekar JJ, Van Zijl PC. 2004. Sustained poststimulus elevation in cerebral oxygen utilization after vascular recovery. J Cereb Blood Flow Metab 24:764–770.

Madsen PL, Hasselbalch SG, Hagemann LP, Olsen KS, Bulow J, Holm S, Wildschiodtz G, Paulson OB, Lassen NA. 1995. Persistent resetting of the cerebral oxygen/glucose uptake ratio by brain activation: evidence obtained with the Kety-Schmidt technique. J Cereb Blood Flow Metab 15:485–491.

Mangia S, Tkac I, Gruetter R, Van De Moortele PF, Giove F, Maraviglia B, Ugurbil K. 2006. Sensitivity of single-voxel ^{1}H-MRS in investigating the metabolism of the activated human visual cortex at 7 T. Magn Reson Imag 24:343–348.

Mangia S, Tkac I, Gruetter R, Van de Moortele PF, Maraviglia B, Ugurbil K. 2007. Sustained neuronal activation raises oxidative metabolism to a new steady-state level: evidence from ^{1}H NMR spectroscopy in the human visual cortex. J Cereb Blood Flow Metab 27:1055–1063.

Mekle R, Mlynarik V, Gambarota G, Hergt M, Krueger G, Gruetter R. 2009. MR spectroscopy of the human brain with enhanced signal intensity at ultrashort echo times on a clinical platform at 3T and 7T. Magn Reson Med 61:1279–1285.

Merboldt KD, Bruhn H, Hanicke W, Michaelis T, Frahm J. 1992. Decrease of glucose in the human visual cortex during photic stimulation. Magn Reson Med 25:187–194.

Mlynarik V, Gambarota G, Frenkel H, Gruetter R. 2006. Localized short-echo-time proton MR spectroscopy with full signal-intensity acquisition. Magn Reson Med 56:965–970.

Mlynarik V, Gambarota G, Xin L, Gruetter R. 2007. Precision of metabolite concentrations obtained by LCModel as a function of the signal-to-noise ratio in rodent brain. ISMRM Fifteenth Scientific Meeting. Berlin: International Society of Magnetic Resonance in Medicine. p 3173.

Olavarria JF, DeYoe EA, Knierim JJ, Fox JM, van Essen DC. 1992. Neural responses to visual texture patterns in middle temporal area of the macaque monkey. J Neurophysiol 68:164–181.

Prichard J, Rothman D, Novotny E, Petroff O, Kuwabara T, Avison M, Howseman A, Hanstock C, Shulman R. 1991. Lactate rise detected by ^{1}H NMR in human visual cortex during physiologic stimulation. Proc Natl Acad Sci USA 88:5829–5831.

Provencher SW. 1993. Estimation of metabolite concentrations from localized in vivo proton NMR spectra. Magn Reson Med 30:672–679.

Reinert KC, Gao W, Chen G, Ebner TJ. 2007. Flavoprotein autofluorescence imaging in the cerebellar cortex in vivo. J Neurosci Res 85:3221–3232.

Rothman DL, Behar KL, Hyder F, Shulman RG. 2003. In vivo NMR studies of the glutamate neurotransmitter flux and neuroenergetics: implications for brain function. Annu Rev Physiol 65:401–427.

Sandor PS, Dydak U, Schoenen J, Kollias SS, Hess K, Boesiger P, Agosti RM. 2005. MR-spectroscopic imaging during visual stimulation in subgroups of migraine with aura. Cephalalgia 25:507–518.

Sappey-Marinier D, Calabrese G, Fein G, Hugg JW, Biggins C, Weiner MW. 1992. Effect of photic stimulation on human visual cortex lactate and phosphates using ^{1}H and ^{31}P magnetic resonance spectroscopy. J Cereb Blood Flow Metab 12:584–592.

Sirotin YB, Das A. 2010. Spatial relationship between flavoprotein fluorescence and the hemodynamic response in the primary visual cortex of alert macaque monkeys. Front Neuroenergetics 2:6.

Tkac I, Gruetter R. 2005. Methodology of H NMR spectroscopy of the human brain at very high magnetic fields. Appl Magn Reson 29:139–157.

Vafaee MS, Gjedde A. 2000. Model of blood–brain transfer of oxygen explains nonlinear flow–metabolism coupling during stimulation of visual cortex. J Cereb Blood Flow Metab 20:747–754.

Vafaee MS, Gjedde A. 2004. Spatially dissociated flow–metabolism coupling in brain activation. Neuroimage 21:507–515.

van der Zwaag W, Marques JP, Hergt M, Gruetter R. 2009. Investigation of high-resolution functional magnetic resonance imaging by means of surface and array radiofrequency coils at 7 T. Magn Reson Imag 27:1011–1018.

Wandell BA, Dumoulin SO, Brewer AA, editors. 2009. Visual cortex in humans. Oxford: Academic. p 251–257.

Wey HY, Wang DJ, Duong TQ. 2011. Baseline CBF, and BOLD, CBF, and CMR_{O2} fMRI of visual and vibrotactile stimulations in baboons. J Cereb Blood Flow Metab 31:715–724.

Yacoub E, Ugurbil K, Harel N. 2006. The spatial dependence of the poststimulus undershoot as revealed by high-resolution BOLD- and CBV-weighted fMRI. J Cereb Blood Flow Metab 26:634–644.

Zeki S. 1990. Parallelism and functional specialization in human visual cortex. Cold Spring Harbor Symp Quant Biol 55:651–661.

Zeki S. 2003. Improbable areas in the visual brain. Trends Neurosci 26:23–26.

Zhu XH, Chen W. 2001. Observed BOLD effects on cerebral metabolite resonances in human visual cortex during visual stimulation: a functional ^{1}H MRS study at 4 T. Magn Reson Med 46:841–847.

Zhu XH, Zhang N, Zhang Y, Ugurbil K, Chen W. 2009. New insights into central roles of cerebral oxygen metabolism in the resting and stimulus-evoked brain. J Cereb Blood Flow Metab 29:10–18.